Metal-Metal Bonding in Late Transition-Metal [M_2L_5] Complexes: Exploring the Limits of the Isolobal Analogy between the CO and AlCp* Ligands

Julius Hornung, Maximilian Muhr, Max Schutz, Patricia Heiß, Johannes Stephan, Christian Jandl, Christian Gemel, Samia Kahlal, Jean-Yves Saillard, Roland A. Fischer

Metal-Metal bonding in late transition-metal [M_2L_5] complexes: Exploring the limits of the isolobal analogy between the CO and AlCp* ligands.

Julius Hornung[#,a] Maximilian Muhr[#,a] Max Schütz,[a] Patricia Heiß,[a] Johannes Stephan,[a] Christian Jandl,[a] Christian Gemel,[a] Samia Kahlal,[b] Jean-Yves Saillard*[,b] and Roland A. Fischer*[,a]

[a] Technical University of Munich, Department of Chemistry and Catalysis Research Center, Chair of Inorganic and Metal-Organic Chemistry, Lichtenbergstr. 4, 85748 Garching, Germany. E-mail: roland.fischer@tum.de

[b] Univ Rennes, CNRS, ISCR-UMR 6226, F-35000 Rennes, France. E-mail: jean-yves.saillard@univ-rennes1.fr

[#] J.H. and M.M. contributed equally.

Abstract

Late dinuclear transition-metal (especially group 10 and 11) homoleptic carbonyl complexes are elusive species and have so far not been isolated. A typical example is the 30-electron species [$Ni_2(CO)_5$], the structure and bonding of which being still debated. We show that, by using the AlCp* ligand (isolobal to CO) it is possible to isolate and fully characterize [$Ni_2(AlCp^*)_5$] (**1**), which inspired us to revisit by DFT calculations the bonding situation within [Ni_2L_5] (L = CO, AlCp*) and other isoelectronic species. The short Ni-Ni X-ray distance in **1** (2.270 Å) should not be attributed to the existence of a typical localized triple-bond between the metals, but rather to a strong through-bond interaction involving the three bridging ligands *via* their donating lone pairs *and* accepting π* orbitals. In contrast in the isostructural 32-electron [$Au_2(AlCp^*)_5$] (**2**) cluster an orbital with M-M antibonding and Al…Al bonding character is occupied, which is in accordance with the particularly long Au-Au distance (3.856 Å) and rather short Al…Al contacts between the bridging ligands (2.843 Å). This work shows that, unlike late transition-metal [$M_2(CO)_x$] species, stable [$M_2(AlCp^*)_x$] complexes can be isolated, owing to the subtle differences between CO and AlCp*. We propose a similar approach for rationalizing the bonding in the emblematic 34 electron species [$Fe_2(CO)_9$].

Keywords: Nickel, Gold, AlCp* Ligand, Metal-Metal Bonding, DFT calculations, Carbonyl Cluster.

Introduction

Investigating the metal-metal interaction in dinuclear transition metal (TM) complexes has a rich history and is a matter of debate until today.[1-7] A prominent example is $Fe_2(CO)_9$, in which each Fe atom has 17 valence electrons (VE) thus suggesting a (still disputed) single Fe-Fe bond in order to fulfill the 18 VE rule for the Fe centers.[8-21] It should be noted that the generally assumed non-existence of a direct Fe-Fe bond in this complex has been explained by using a representation that describes one of the three bridging CO ligands as being involved in 3-center/2-electron bonds, thus allowing the metal centers to reach the 18 VE configuration (see Figure S8).[22] While $Fe_2(CO)_9$ is synthetically easily accessible[23], therefore giving access to experimental data that can be confronted to computed compounds, such data are more difficult to access for, e.g., dinuclear Ni-carbonyl compounds $Ni_2(CO)_x^z$.[24] On this point, it is of note that the isolable 17 VE $[Ni(CO)_4]^+$ radical does not dimerizes.[25] Spectroscopic data are however available for selected charged clusters, which were studied in Kr matrices[26] or in the gas phase[27]. Accessing the neutral $Ni_2(CO)_x$ (x = 5, 6, 7) on a macroscopic scale still remains elusive. Following the 18 VE rule the compounds are predicted to comprise a Ni-Ni single (for x = 7), double (for x = 6) and a triple (for = 5) bond. Recently Liu and coworkers re-investigated the Ni-Ni bonding in $[Ni_2(CO)_5]$ and found major contributions of the three bridging CO ligands that was interpreted in terms of triple 3-center/2-electron Ni-C-Ni bonding.[28] This delocalized representation allows the Ni centers to attain the 18-electron configuration without assuming any direct metal-metal bond (Scheme 1).[22] TM containing compounds and especially multiple TM-TM bonds are of fundamental interest and may be viewed as building blocks for larger clusters or even surfaces.[29, 30] Textbook examples are the quadruple bond containing compounds $Re_2Cl_8^{2-}$ (unbridged)[31] and $Mo_2(acetate)_4$ (bridged)[32], which are hold together by one σ-, two π- and one δ-interactions.[33, 34] Tailor-made terphenyl ligands even allow for a quintuple Cr-Cr bond (unbridged)[35], so do bulky amidinate ligands support a quintuple Mo-Mo bond (bridged)[36-38]. The choice of ligands plays a crucial role: ligand-to-metal bonds compete with metal-metal bonding for available TM valence orbitals.[39] At the same time, ligands are necessary to protect TM-TM multiple bonds and avoid the involved electrons to participate in reactions like cluster growth.

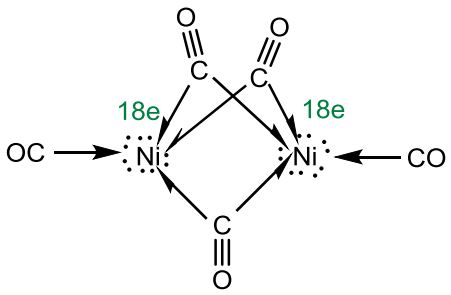

Scheme 1. The Lewis representation of $[Ni_2(CO)_5]$ proposed by Liu *et al.*[28] and using the half-arrow representation of Green *et al.*,[22] in which each μ-CO lone pair is represented by a pair of half-arrows. In this representation, each bridging carbonyl may be regarded as effectively contributing two electrons to the electron count of both nickel atoms.

We are typically interested in intermetalloid clusters of the general formula $[TM_aE_b](R)_c$ (E = group 13 metal; R = organic rest), their reactivity and bonding.[40-46] ECp* units have been proven to be good ligands in these class of compounds, ranging from small complexes like $[Ni(AlCp^*)_4]$[47] to true superatoms with emerging conductive band such as $[Cu_{43}(AlCp^*)_{12}]$[48]. The ER ligands have been shown to be isoelectronic/isolobal[49, 50] to CO and phosphines, by extensive substitution chemistry studies[44, 51, 52], as well as by theoretical investigations[53-55]. ER ligands have been electronically compared to CO by Frenking, e.g. in homoleptic $[Ni(ER)_4]$ as well as heteroleptic $[(CO)_3Ni(ER)]$.[54, 55] These studies conclude that the main covalent bonding contribution of ER ligands is σ-donation (Ni←ER), whereas the π-back-donation (Ni→ER) remains small (for E = Al, Ga, In, Tl) and stands in sharp contrast to the textbook π-acceptor CO. Notably, electrostatic interactions were identified as major bonding contributions, especially in homoleptic $[Ni(ER)_4]$ complexes, making the Ni-E bond a strongly polarized bond.[55] Irrespective of the details in differences, in general CO and ER share the same bonding principles towards TMs.

A vivid example of this relationship is the dinuclear $[(Cp^*Ga)_2Pt_2(\mu^2\text{-}GaCp^*)_3]$, which can be viewed as an analogue of the thermally unstable $[Pt_2(CO)_5]$.[56] Especially the structural motive $TM_2(\mu^2\text{-}ER)_3$ in which two TMs are bridged by three ER ligands frequently occurs in such compounds.[44, 56-58] We were therefore interested in gaining a deeper understanding of the TM-TM interactions in clusters exhibiting such a structural motif. In this report we present two such compounds representing extreme situations of TM-TM bonding: $[(Cp^*Al)_2Ni_2(\mu^2\text{-}AlCp^*)_3]$ (**1**) with a short Ni-Ni distance and $[(Cp^*Al)_2Au_2(\mu^2\text{-}AlCp^*)_3]$ (**2**) with a very long

Au…Au separation. The bonding situation in both complexes is discussed and compared to the parent $[Ni_2(CO)_5]$, which is synthetically not accessible.

1. Results and discussion

1.1 Synthesis, characterization and X-ray structure of $[M_2(AlCp^*)_5]$ (M = Ni, Au).

1.1.1 $[Ni_2(AlCp^*)_5]$

Treatment of a toluene solution of $[Ni_2(dvds)_3]$ (dvds = 1,1,3,3-Tetramethyl-1,3-divinyldisiloxane) with six equivalents of AlCp* (Cp* = 1,2,3,4,5-Pentamethylcyclopentadienyl) at 70°C results in color change from orange to deep red after several minutes. After 2h, LIFDI-MS measurements indicate complete consumption of the starting material $[Ni_2(dvds)_3]$ and the formation of $[Ni(AlCp^*)_4]$[47] as the main product together with a small amount of the title compound $[Ni_2(AlCp^*)_5]$ (**1**). Recrystallisation from *n*-hexane affords $[Ni_2(AlCp^*)_5]$ in pure form. From the concentrated reaction solution, $[Ni_2(AlCp^*)_5]$ deposits as a red crystalline solid after storing for several days at 8 °C. LIFDI-MS measurement of the isolated compound confirms the crystallization of $[Ni_2(AlCp^*)_5]$, showing the $[M]^+$ ion peak at m/z [a.u.] = 926 with the expected isotopic pattern (Figure S4-5). The ^{1}H-NMR of the isolated product **1** in C_6D_6 (Figure S1-2) exhibits two signals in the expected range for Ni-AlCp* protons[41, 44, 47, 51, 59, 60] at 2.01 and 1.97 ppm with a signal ratio of 2:3 indicating the existence of two distinct AlCp* groups (terminal and bridging). ^{1}H-NMR measurements at elevated temperatures (90°C in toluene-d_8) does not lead to a coalescence of these signals. The ^{13}C-NMR signals (Figure S3) are in accordance to the ^{1}H-NMR showing two sets of signals for the distinct AlCp* groups. Single crystal X-Ray measurement unambiguously verifies the isolation of $[Ni_2(AlCp^*)_5]$. Indeed, **1** is isostructural to the already known $[TM_2(ECp^*)_5]$[44] (TM = Pd, Pt; E = Al, Ga) compounds and the predicted structure of the hypothetical $[Ni_2(CO)_5]$[5, 28], having three bridging and two terminal ligands at the central Ni-dimer (Figure 1). The Ni-Ni distance of 2.2702 Å is considerably shorter (about 8%) than twice the covalent radius of Ni (2.48 Å)[61] and only slightly longer than the predicted Ni-Ni distance in $[Ni_2(CO)_5]$ (2.18 Å),[28] hinting to the presence of significant Ni-Ni interactions. The Ni-AlCp*$_{terminal}$ distances of 2.2309(16) Å are in the range of other Ni-AlCp* distances[41, 44, 47, 51, 59, 60], whereas the Ni-AlCp*$_{bridging}$ distance is with 2.31 Å (average) slightly longer. The Al-Cp*$_{centroid}$ distances are independent of the bonding mode of the AlCp* ligands and with about 1.94 Å comparable to literature known values.

Table 1. Selected averaged interatomic distances (Å) and bond angles (°) in $[Ni_2(AlCp^*)]_5$ and $[Au_2(AlCp^*)]_5$[62]. The experimental X-ray values are on top of their DFT-optimized counterparts in parentheses.

	M-M	M-Al[a]	M-(μ-Al)[a]	Al… Al[a]	M-(μ-Al)-M[a]	Al-M-(μ-Al)[a]	(μ-Al)-M-(μ-Al)[a]
$[Ni_2(AlCp^*)]_5$	2.270 (2.286)	2.231 (2.203)	2.317 (2.292)	3.497 (3.437)	58.7 (59.8)	119.3 (119.9)	98.0 (97.2)
$[Au_2(AlCp^*)]_5$	3.856 (3.884)	2.392 (2.408)	2.532 (2.545)	2.843 (2.848)	99.2 (99.5)	139.5 (139.6)	68.3 (68.1)

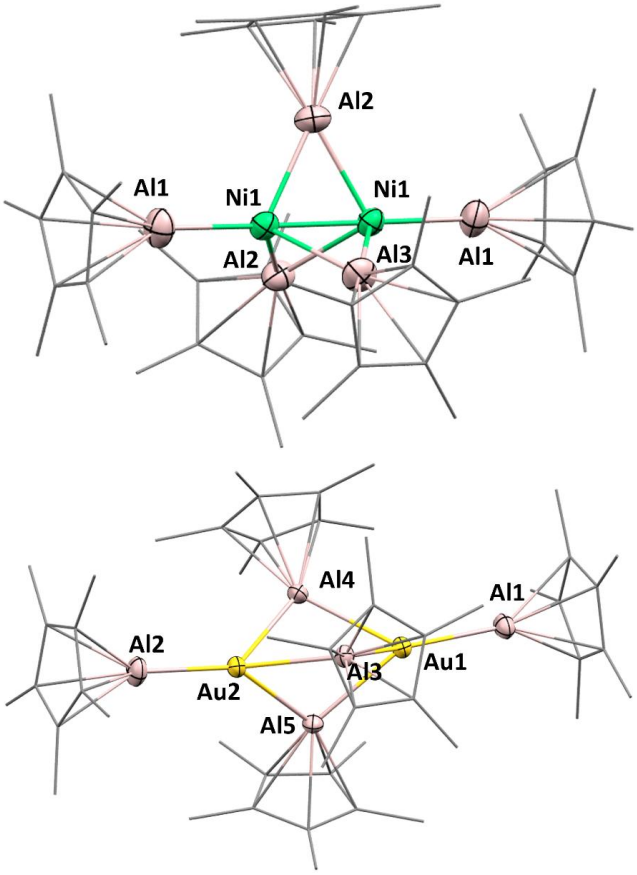

Figure 1. X-ray molecular structures of **1** (top) and **2** (bottom)[62]. Thermal ellipsoids are given at the 50% probability level, Cp* ligands are given in wireframe depiction and H atoms are omitted for clarity. Selected averaged bond lengths [Å] and angles [°] are provided in Table 1.

1.1.2 $[Au_2(AlCp^*)_5]$

The synthesis of $[Au_2(AlCp^*)_5]$ (**2**) can be realized from treatment of ^{i}DippAuH (^{i}Dipp = 2,3-dihydro-1,3-bis(2,6-diisopropylphenyl)-1H-imidazol-2-ylidene) with excess of AlCp* (2.5 eq.) in toluene after prolonged reaction times (18 h). Exact procedure (see SI) as well

as spectroscopic details have recently been described elsewhere.[62] The crystal structure (Figure 1) of $[Au_2(AlCp^*)_5]$ (**2**) is related to that of **1**: A central Au-Au unit is bridged by three AlCp* units and flanked by one terminal AlCp* per Au atom. Striking differences are noted in the bond lengths: The TM-TM distance (3.856 Å) is severely elongated compared to **1** and far from twice the Au covalent radius (2.72 Å)[61]. On the other hand, the Al-Al distances of the bridging AlCp* units are significantly shortened by about 0.6 Å compared to **1**. Important bond distances and angles can be found in Table 1, the synthesis protocol and further spectroscopic data of **2** were recently published.[62]

2.2 Computational and bonding analysis

Before entering into the details of our orbital analyses below, we would like to mention that our optimized geometries of $[Ni_2(AlCp^*)_5]$ and $[Au_2(AlCp^*)_5]$ are in good agreement with their X-ray structures. Their major metrical data are compared in Table 1 above.

2.2.1 The nickel carbonyl reference $[Ni_2(CO)_5]$

Assuming a localized 2-center/2-electron bonding scheme for $[Ni_2(CO)_5]$, with 2x10 + 5x2 = 30 valence electrons, the 18-electron rule predicts for this complex a formal Ni-Ni bond order of (2x18 - 30)/2 = 3, to which the Lewis formula **I** (Scheme 2) can be associated. This compound has been investigated at the DFT level by King and coworkers.[5] They found the expected $[(CO)Ni(\mu\text{-}CO)_3Ni(CO)]$ D_{3h} ground state structure, with a Ni-Ni distance of 2.19 Å that does not completely exclude the existence of a (weak) triple bond. They also predicted that $[Ni_2(CO)_5]$ would be surprisingly stable with respect to dissociation. More recently, a comprehensive theoretical analysis by Liu *et al.*[28] of the $[Ni_2(CO)_5]$ electronic structure, also based on DFT calculations, ended up with the convincing conclusion that there is no formal metal-metal triple bond in this molecule. Rather, they describe the Ni-Ni bonding interaction as resulting from a delocalization of three 2-electron/3-center Ni-C-Ni bonds, originating from the donation of the three μ-CO lone pairs (Scheme 1). In the following, we would like to throw a related but somewhat different light on the problem, by using in a first step a qualitative model based on symmetry arguments and frontier orbital interactions.

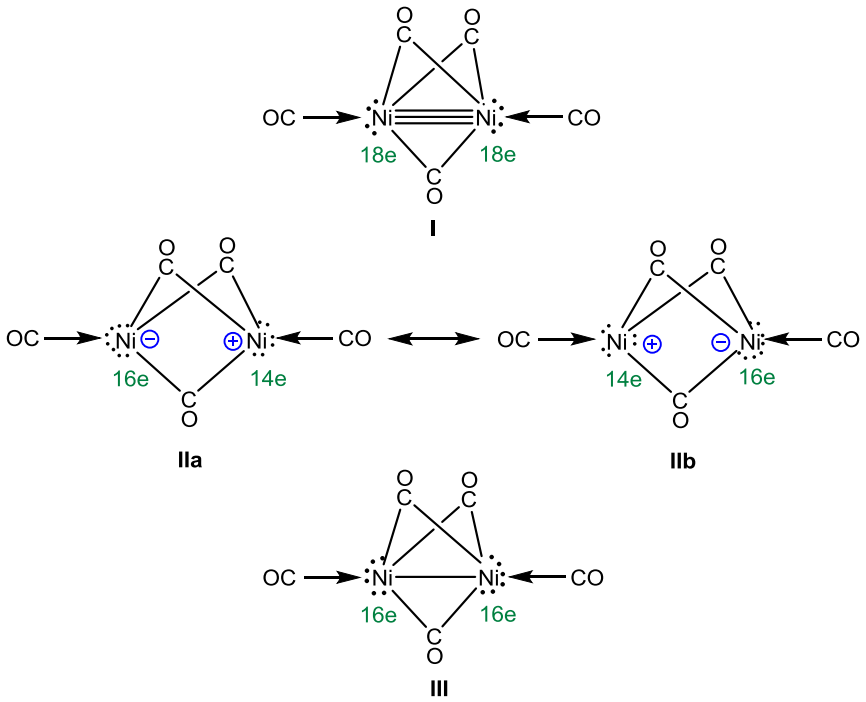

Scheme 2. Putative Lewis structures for $[Ni_2(CO)_5]$. Top: With a metal-metal triple bond; middle: With no metal-metal bond; bottom: With a metal-metal single bond.

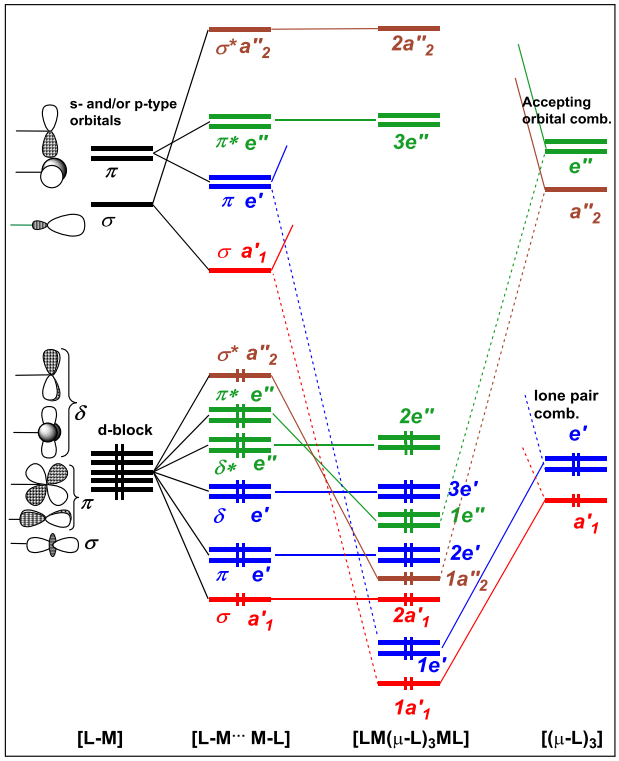

Figure 2. Simplified interaction MO diagram for a 30-electron $[LM(\mu\text{-}L)_3ML]$ ($M = d^{10}$) complex of D_{3h} symmetry. Only the 2-electron/2-orbital bonding interactions are considered. The energy ordering of the occupied/vacant levels is arbitrary.

Following the early approach of Summerville and Hoffmann,[20] a qualitative bonding description of $[Ni_2(CO)_5]$ can be developed starting from the crude MO diagram sketched in Figure 2, which illustrates the interaction between the [L-M…M-L] and $[(\mu\text{-L})]_3$ fragments in a 30-electron $[M_2L_5]$ complex, assuming ideal D_{3h} symmetry. It represents only the stabilizing 2-orbital/2-electron interactions, *i.e.*, those involving one occupied (donor) and one vacant (accepting) orbital, which are those principally associated with the bonding between the two fragments. For the sake of simplicity, second-order intermixing between several orbitals of the same symmetry are neglected in this first step. Assuming M = Ni and L = CO in Figure 2, the [(CO)-Ni…Ni-(CO)] frontier orbitals are the in-phase and out-of-phase combinations of the five 3d(Ni) AOs, the two $4p_\pi$(Ni) AO's and the 4s/4p(Ni) hybrids of a single (CO)-Ni linear fragment (left side of Figure 2).[63] The frontier orbitals of the $(\mu\text{-CO})_3$ fragment are the combinations of the three σ-lone pairs ($a'_1 + e'$) and the three π*(CO) orbitals which are parallel to the Ni-Ni vector. The three other π*(CO) orbitals, perpendicular to the Ni-Ni vector, are principally involved in C=O bonding and thus not considered at this stage of the analysis. They combine in $e' + a'_2$. The carbonyl $a'_1 + e'$ lone pair combinations interact in a bonding way with the vacant sp(Ni) and $4p_\pi$(Ni) combinations of the same symmetry. The vacant $a''_2 + e''$ π*(CO) combinations interact in a bonding way with the occupied 3d(Ni) combinations of π* and σ* nature. As a result, six occupied metal-ligand bonding MOs are built ($1a'_1 + 1e' + 1a''_2 + 1e''$), to which are corresponding six antibonding vacant counterparts. These six bonding electron pairs are associated with the six Ni-(μ-CO) bonds. The other occupied MOs of $[Ni_2(CO)_5]$ are non-bonding with respect to metal-ligand interactions, but with respect to Ni-Ni interactions they are of σ ($2a_1$) , π ($2e'$), δ ($3e'$) and δ* ($2e''$) character. Whereas the occupation of both δ and δ* cancels δ bonding if any (four δ-type lone pairs), one may wonder about σ and π bonding. Within a localized 2-center/2-electron scheme, the existence of one σ and two π bonds would require that of vacant σ* and π* MOs, associated, together with their occupied bonding counterparts, to the corresponding three metal-metal bonding electron pairs. It turns out that this is not the case since the σ* and π* counterparts are formally occupied and participate in metal-ligand bonding. Thus, the electrons occupying the 3d-type levels of σ ($2a'_1$) and π ($2e'$) character should be rather considered as metal lone pairs. It follows that, from the strict point of view of a localized 2-center/2-electron bonding description, the MO diagram of Figure 2 should correspond to Lewis structure(s) in which no Ni-Ni bond exists. The resonant formulae **IIa** and **IIb** (Scheme 2), with 15-electron metal centers in average, can thus be proposed.

One may however argue that the high-lying vacant *3e"* and *2a"*$_2$ MOs of Figure 2, not involved in the bonding with the μ-CO ligands, are in fact the "missing" σ* and π* vacant counterparts of the occupied σ (2*a'*$_1$) and π (2*e'*) levels, thus completing the MO panel for a localized Ni-Ni triple bond. It turns out that our calculations do not support this view, as discussed a little later. Substantial through-bond Ni-Ni interactions are however expected, originating from the mixing of the occupied σ* (*a"*$_2$) and π* (*e"*$_2$) orbitals of [(CO)-Ni…Ni-(CO)] with their ligand counterparts (Figure 2). This mixing leads to partial depopulation of these metal-metal antibonding levels, thus creating some Ni-Ni bonding. A similar effect is expected from the mixing of the vacant σ (*a'*$_1$) and π (*e'*) levels of [(CO)-Ni…Ni-(CO)] with the CO lone pair combinations, leading to partial population of these Ni-Ni bonding orbitals. Introducing now in a following step intermixing between several orbitals of same symmetry (in particular the non-negligible π/δ and π*/δ* mixings), supplementary Ni-Ni bonding is predicted. Moreover, the *e'*$_\perp$ combinations of the three π*(CO) orbitals which are associated to C=O bonding (perpendicular to the Ni-Ni vector, not represented in Figure 2), are also expected to somewhat participate to bonding interactions with occupied 3d levels, contributing also to Ni-Ni bonding. Their *a'*$_{2\perp}$ congener, not involved in any interaction with the metals remains unperturbed, lying at high energy (not shown in Figure 2).

Table 2. Occupation of the frontier orbitals of the [L-M…M-L] and $[(\mu\text{-L})]_3$ fragments in selected $[M_2L_5]$ (M = Ni, Pt, Au) complexes of D_{3h} symmetry (L = CO) or approximate D_{3h} symmetry (L = AlCp). From Mulliken population analysis (see Computational Details).

		$[Ni_2(CO)_5]$ (D_{3h})	**$[Pt_2(CO)_5]$ (D_{3h})**	**$[Ni_2(AlCp)_5]$ (pseudo-D_{3h})**	**$[Au_2(AlCp)_5]$ (pseudo-D_{3h})**
[L-Ni…Ni-L] fragment orbitals	IR[a] in D_{3h} symmetry				
σ* (sp)	a''_2	0.02	0.02	0.03	1.36
π* (4p)	e''	0.20	0.14	0.05	0.07
π (4p)	e'	1.14	1.08	1.04	0.63
σ (sp)	a'_1	0.66	0.93	1.16	0.90
σ* (3d)	a''_2	1.58	1.55	1.69	1.83
δ* (3d)	e''	3.67	3.69	3.75	3.84
π* (3d)	e''	3.83	3.82	3.90	3.92
δ (3d)	e'	3.42	3.45	3.53	3.88
π (3d)	e'	3.76	3.84	3.75	3.91
σ (3d)	a'_1	1.94	1.65	1.62	1.80
$[\mu\text{-L}]_3$ fragment orbitals	IR[a] in D_{3h} symmetry				
$\pi_{//}$(accepting)	e''	0.32	0.38	0.14	0.12
$\pi_{\perp}$ (accepting)	e'	0.48	0.41	0.34	0.61
($\pi_{//}$(accepting)	a''_2	0.48	0.49	0.45	1.22
e' (lone pairs)	e'	3.18	3.25	2.86	3.22
a'_1 (lone pairs)	a'_1	1.46	1.40	1.50	1.23

[a] IR = irreducible representation (see Figure 1).

More quantitatively, we have evaluated the above-discussed interactions by computing the populations of the fragment orbitals through a fragment interaction analysis based on DFT calculations at the BP86-ZORA/TZ2P/D3(BJ) level (see computational details). The occupation of the fragment orbitals discussed above are summarized in Table 2. It appears from these values that in $[Ni_2(CO)_5]$ the occupation of the σ and π Ni-Ni bonding orbitals of the metallic fragment overpasses those of the antibonding ones by 1.0 and 0.9 electron respectively. In particular, substantial bonding is induced by the occupation of the diffuse σ(sp) (a'_1) and π(4p) (e') levels. Although significant, these values are far from the limit values corresponding to an ideally localized Ni≡Ni bond (2 and 4, respectively). They also differ from what one would expect for a single bond (2 and 0, respectively) corresponding to the Lewis structure **III** in Scheme 2. Consistently, the computed Ni-Ni Wiberg index (0.097, see Table 3) is indicative of a weak bonding interaction. As already shown by Liu *et al.*[28] in their QTAIM analysis of the electron density, the indicators associated with the Ni-Ni bond critical point (bcp) are also in line with a weak Ni-Ni bonding character (Table 4).

In order to test the stability of our bonding description within the group 10 triad, we also computed the hypothetical $[Pt_2(CO)_5]$ relative. The corresponding results gathered in Tables 2-4 confirm the similarities between both Ni and Pt species, with a (moderately) stronger metal-metal covalent bonding in the case of Pt.

Table 3. Selected computed data for the $[M_2L_5]$ (M = Ni, Pt, Au; L = CO, AlCp, AlCp*) complexes.

	$[Ni_2(CO)_5]$ (D_{3h})	**$[Pt_2(CO)_5]$ (D_{3h})**	**$[Ni_2(AlCp)_5]$ (C_s)**	**$[Ni_2(AlCp^*)_5]$ (C_1)**	**$[Au_2(AlCp)_5]$ (C_s)**	**$[Au_2(AlCp^*)_5]$ (C_1)**
M-M (Å) [WBI]	2.178 [0.097]	2.593 [0.123]	2.234 [0.095]	2.286 [0.102]	3.813 [0.064]	3.884 [0.049]
L…L (Å) [a] [WBI]	2.874 [0.107]	3.058 [0.083]	3.482 [0.328]	3.437 [0.374]	3.006 [0.579]	2.848 [0.715]
HOMO-LUMO gap (eV)	2.72	2.93	2.32	2.16	2.13	1.86
M NAO charge [a]	0.33	0.33	-0.37	-0.47	-0.03	-0.01
M-M Wiberg bond index	0.097	0.123	0.095	0.102	0.064	0.049

[a] Averaged values in the case of L = AlCp and AlCp*.

Table 4. QTAIM descriptors of the M-M bond in the $[M_2L_5]$ (M = Ni, Pt, Au; L = CO, AlCp, AlCp*) complexes.

Compound		$[Ni_2(CO)_5]$	$[Pt_2(CO)_5]$	$[Ni_2(AlCp)_5]$	$[Ni_2(AlCp^*)_5]$	$[Au_2(AlCp^*)_5]$
Atom charge[a]	M	0.439	0.249	-1.432	-1.448 [avg.]	-1.778[avg.]
Delocalisation index	δ	0.454	0.559	1.046	1.021	0.430
bcp indicators[b]	ρ	0.079	0.073	0.077	0.071	-
	$\nabla^2\rho$	0.171	0.108	0.152	0.128	-
	H	-0.027	-0.028	-0.027	-0.025	-
	V	-0.097	-0.082	-0.093	-0.081	-
	$\lvert V \rvert / G$	1.389	1.507	1.418	1.435	-

[a] Averaged values in the case of L = AlCp and AlCp*.
[b] ρ , $\nabla^2\rho$, H, V and G are the electron density, Laplacian of density, energy density, potential energy density and kinetic energy density values at the bcp, respectively. All values in a.u.

2.2.2 $[Ni_2(AlCp)_5]$ and $[Ni_2(AlCp^*)_5]$

The isolobal analogy between CO and AlCp* is illustrated in Figure 3. Both ligands possess a similar set of frontier orbitals: One occupied donor orbital that contains a σ lone pair, and two degenerate vacant accepting orbital which are of π type with respect to the ligand rotational axis. They are the π*(CO) orbitals of the former and the σ*(Al-C_5) orbitals

of e_1 symmetry in the later (assuming C_{5v} symmetry). There is however an important difference between the two ligands, namely their size. With its five methyl substituents on the C_5 ring, AlCp* is much bulkier, generating steric and van der Waals interactions between neighboring ligands that often lower the symmetry of the complex.

In order to keep as close as possible to D_{3h} symmetry, we first investigated the simplified $[Ni_2(AlCp)_5]$ model, of actual C_s symmetry, but which can be reasonably considered as pseudo-D_{3h}. Its corresponding data in Table 2 are close to those found for $[Ni_2(CO)_5]$. In particular, the occupation of the σ and π Ni-Ni bonding orbitals of the metallic fragment overpasses those of the antibonding ones by 1.1 and 0.8 electron respectively. The occupations of the ligand frontier orbitals indicate that AlCp is a better σ-donor and lesser π-acceptor than CO, but the differences are not very large. Despite the Ni-Ni distance is larger by ~ 0.1 Å in the AlCp complex, the corresponding Wiberg index is slightly larger (Table 3). The corresponding QTAIM bcp indicators of the two complexes are also quite similar (Table 4). The major difference between them is the polarity of the Ni-L bonds,[55] which is substantial in the L = AlCp case, the metal becoming negatively charged (Tables 3 and 4). The real $[Ni_2(AlCp^*)_5]$ complex is too far from D_{3h} symmetry for allowing a sufficiently accurate orbital occupation analysis as those provided in Table 1. Nevertheless, its computed data in Table 3 indicate similar bonding features as that found for its simplified $[Ni_2(AlCp)_5]$ model. The hypothetical $[Pt_2(AlCp^*)_5]$ also provided similar results, in full consistency with those of the strongly related and isolated $[Pt_2(GaCp^*)_5]$.[56]

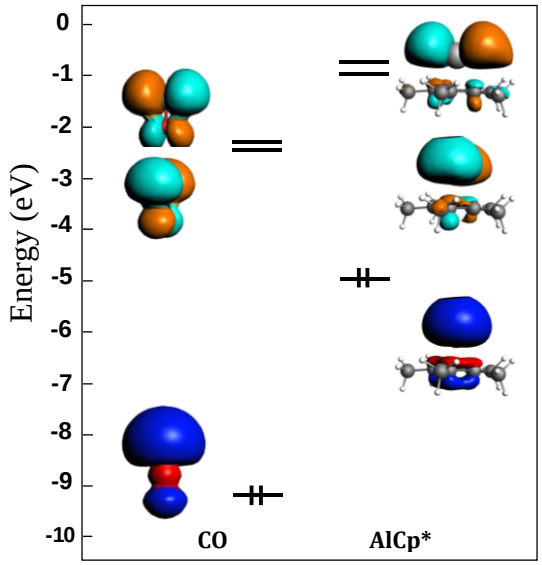

Figure 3. The frontier orbitals of the CO and AlCp* ligands.

2.2.3 $[Au_2(AlCp)_5]$ and $[Au_2(AlCp^*)_5]$

The 18-electron rule predicts a formal Au-Au bond order of (2x18 - 32)/2 = 2 for the 32-electrons $[Au_2(AlCp^*)_5]$. This is obviously not the case, owing to the observed Au…Au non-bonding distance of 3.856 Å. In order to solve this puzzle, and as for the nickel relative above, we first investigated the simplified $[Au_2(AlCp)_5]$ model in order to maintain a sufficiently approximate D_{3h} symmetry. Surprisingly, our optimized structure was found highly distorted. Removing Grimme's empirical corrections for dispersion forces,[64, 65] yielded the expected C_s (pseudo- D_{3h}) structure. Discarding Grimme's corrections provides generally larger interatomic distances, but we found this hypothetical model to be sufficiently accurate for providing a good orbital rationalization. The corresponding computed data are gathered in Tables 2-3. They indicate that the two electrons that are formally added when going from $[Ni_2L_5]$ (30-electron) to $[Au_2L_5]$ (32-electron) occupy an orbital of a''_2 pseudo-symmetry which is Au-Au antibonding and Al-Al bonding. For reasoning purpose, let's assume that before interaction the two "supplementary" electrons are formally located on the $[(\mu\text{-}L)_3]$ fragment, *i.e.*, in the a''_2 LUMO on the right side of Figure 2. This time, this occupied a''_2 fragment orbital cannot interact in a stabilizing way with the occupied a''_2 (σ^*) d-type combination of the metallic fragment because it is also occupied. Rather, it will seek for a vacant counterpart to set up a 2-electron/2-orbital interaction, that is, the a''_2 (σ^*) hybrid combination. The bonding combination between these two a''_2 fragment orbitals that will result will host the two "supplementary" electrons. Being Au-Au σ-antibonding and Al…Al π-bonding, its occupation induces substantial elongation of the Au…Au vector together with some contraction of the Al_3 triangle. This orbital, the HOMO-2 of $[Au_2(AlCp)_5]$, is plotted in Figure 4 and the whole bonding situation is crudely sketched in Figure 5. The significant participation to the bonding of the a''_2 (σ^*) hybrid combination is clearly perceptible in Table 2. Its partial population cancels the weak bonding interaction that exists in the 30-electron relatives so that no QTAIM bond path between the metals is found. Rather, a cage critical point (ccp) sits in the middle of the Au_2Al_3 trigonal bipyramid. On the other hand, bcp's appear between the Al atoms. A very similar bonding situation is found for the optimized real compound $[Au_2(AlCp^*)_5]$ (Tables 3 and 4), with even shorter Al-Al distances (2.848 Å), due to the reintroduction of dispersion corrections in the calculations, and in good agreement with experiment. It is noteworthy that the hypothetical 30-electron oxidized species $[Au_2(AlCp^*)_5]^{2+}$ restores the (weak) metal-metal interaction (Au-Au = 2.698 Å) and moves the Al atoms away from each other (Al…Al = 3.714 Å). These values are close to that found for the isoelectronic $[Pt_2(AlCp^*)_5]$.

The bonding in $[Au_2(AlCp^*)_5]$ is too much delocalized for being tentatively described by one or several Lewis formulae. We propose to view it as a cluster, the skeletal core of it being the Au_2Al_3 trigonal bipyramid. According to the Wade-Mingos rules[66] the favored electron count associated with such a polyhedral *closo* architecture corresponds to six electron pairs, providing that each of the six fragments participate to the bonding with σ and π frontier orbitals. Clearly, with its six bonding electron pairs of a'_1, e', e'' and a''_2 in ideal D_{3h} symmetry (Figure 2), $[Au_2(AlCp^*)_5]$ can be considered as following the Wade-Mingos rules.

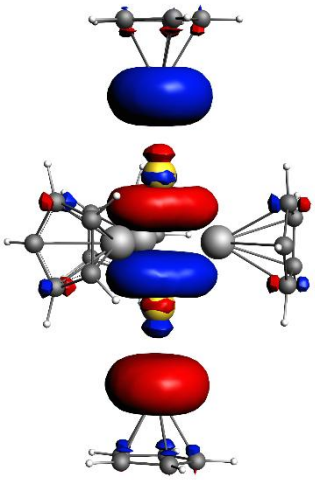

Figure 4. The HOMO-2 of $[Au_2(AlCp)_5]$.

It is of note that a series of isostructural main-group clusters of the type $[E_2(AlCp^*)_5]$ (E = As,[67] Bi,[68] Cp^*AlSi^+ [69] and Cp^*AlGe^+ [69] have been characterized, which have also been described as *closo* species[69] bearing six skeletal electron pairs, despite the fact that some of them[68, 69] exhibit long non-bonding Al…Al contacts. The relationship between the electronic structure of these species and that of $[Au_2(AlCp^*)_5]$ will be the subject of further investigations.

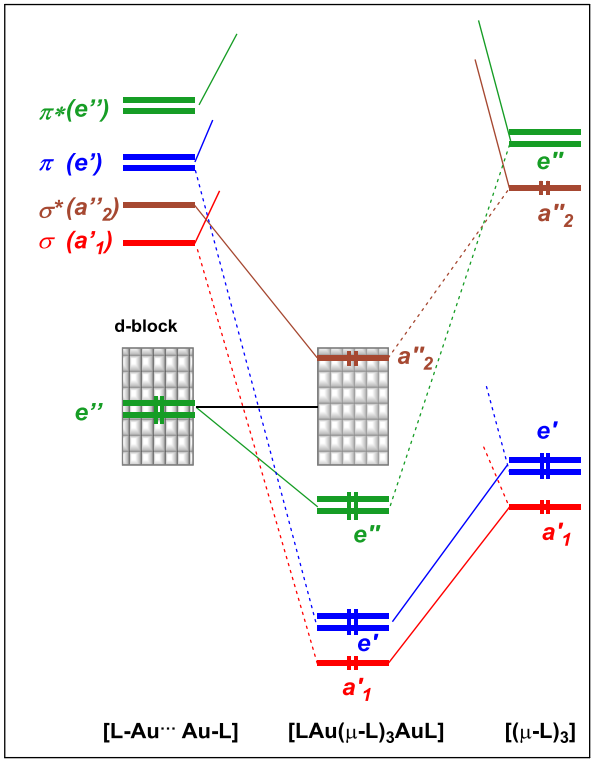

Figure 5. Simplified interaction MO diagram for a 32-electron [LAu(μ-L)$_3$AuL] complex of D_{3h} symmetry. Only the 2-electron/2-orbital bonding interactions are considered. The energy ordering of the occupied/vacant levels is arbitrary.

2. Concluding remarks

The [Ni_2(AlCp*)$_5$] complex reported above is the first fully characterized species isoelectronic to the archetypal although still unknown [$Ni_2(CO)_5$]. Because of the isolobal analogy between CO and AlCp*, both complexes have similar bonding features. We propose to describe their electronic structures by the Lewis formulae **IIa** and **IIb** of Scheme 2, and, at most, with some minor admixture of formula **I** (and perhaps **III**). Indeed, our calculations are consistent with the absence of a localized Ni-Ni bond of any order. Rather, substantial Ni…Ni through-bond interaction occurs *via* the building of the six ligand-Ni bonds. From this point of view, our description is not contradicting that of Liu *et al.*[28] who rationalize Ni-Ni bonding in [$Ni_2(CO)_5$] from the formation of three 2-electron/3-center bonds originating from the donation to the Ni-Ni vector of the three ligand lone pairs, their bonding scheme being represented by the Lewis formula of Scheme 1. However, our calculations suggest that non-negligible Ni-Ni bonding also occurs from metal back-donation to the ligand accepting orbitals. This Ni→L back-donation is also responsible for the building of non-negligible Ni-(μ-L) bonding, which is not accounted for in the formula of Scheme 1. At this point, we also

would like to mention that there is no "*legal*" requirement for a metal center to obey the 18-electron rule. Although most of the stable organometallic TM centers do, counter-examples are not rare.[63] This is why we privilege the classical (fully localized) writing of Lewis formulae as those in Scheme 2, rather than those that allow metals to reach the 18-electron rule by sharing ligand electron pairs through the building of 3-center bonds.[22] It is of note that a similar bonding description in $Fe_2(CO)_9$, with two major resonant Lewis formulae having no formal Fe-Fe bond and exhibiting one 18-electron and one 16-electron metal centers can be proposed[21] (see Figure S8), assuming that the (weak) Fe-Fe bonding character (if any) results from through-bond interaction. Finally, it should be reminded that, although isolobal, CO and AlCp* have differences, in particular with respect to their sizes. This is why a 32-electron species like $[Au_2(AlCp^*)_5]$ cannot exist with CO in the place of AlCp*, since the small size of the carbonyl ligand would not allow for the formation of C…C bonding, together with maintaining a long Au…Au separation. This work demonstrates that the AlCp* ligand is able to stabilize compounds that are not stable with carbonyls and suggests that a new facet of the chemistry of M_xL_y transition-metal complexes and clusters, not reachable with classical isolobal 2-electron carbonyl, phosphine, N-heterocyclic carbenes, isonitriles, … ligands, could be explored with L = AlCp* or related ligands.

3. Acknowledgement

This work was funded by the German Research Foundation (DFG) within a Reinhard Koselleck Project (FI-502/44-1) and supported by the GENCI French National computing resource (grant A0090807367).

4. References

(1) Tiana, D.; Francisco, E.; Macchi, P.; Sironi, A.; Martín Pendás, A. An Interacting Quantum Atoms Analysis of the Metal–Metal Bond in $[M_2(CO)_8]^n$ Systems. *J. Phys. Chem. A* **2015**, *119* (10), 2153-2160. DOI: 10.1021/acs.jpca.5b00070.

(2) Macchi, P.; Sironi, A. Chemical bonding in transition metal carbonyl clusters: complementary analysis of theoretical and experimental electron densities. *Coord. Chem. Rev.* **2003**, *238-239*, 383-412. DOI: https://doi.org/10.1016/S0010-8545(02)00252-7.

(3) Dyson, P. J.; McIndoe, J. S. *Transition Metal Carbonyl Cluster Chemistry*; CRC Press, 2000. DOI: https://doi.org/10.1201/9781315273815

(4) Xie, Y.; Schaefer, H. F.; King, R. B. Binuclear Homoleptic Iron Carbonyls: Incorporation of Formal Iron−Iron Single, Double, Triple, and Quadruple Bonds, $Fe_2(CO)_x$ (x = 9, 8, 7, 6). *J. Am. Chem. Soc.* **2000**, *122* (36), 8746-8761. DOI: 10.1021/ja001162y.

(5) Ignatyev, I. S.; Schaefer, H. F.; King, R. B.; Brown, S. T. Binuclear Homoleptic Nickel Carbonyls: Incorporation of Ni−Ni Single, Double, and Triple Bonds, $Ni_2(CO)_x$ (x = 5, 6, 7). *J. Am. Chem. Soc.* **2000**, *122* (9), 1989-1994. DOI: 10.1021/ja9914083.

(6) Herrmann, W. A. 100 Jahre Metallcarbonyle. Eine Zufallsentdeckung macht Geschichte. *Chem. Unserer Zeit* **1988**, *22* (4), 113-122. DOI: https://doi.org/10.1002/ciuz.19880220402.

(7) Colton, R.; McCormick, M. J. μ_2 Bridging carbonyl systems in transition metal complexes. *Coord. Chem. Rev.* **1980**, *31* (1), 1-52. DOI: https://doi.org/10.1016/S0010-8545(00)80365-3.

(8) Pan, S.; Zhao, L.; Dias, H. V. R.; Frenking, G. Bonding in Binuclear Carbonyl Complexes $M_2(CO)_9$ (M = Fe, Ru, Os). *Inorg. Chem.* **2018**, *57* (13), 7780-7791. DOI: 10.1021/acs.inorgchem.8b00851.

(9) Hogarth, G. The diiron centre: $Fe_2(CO)_9$ and friends. In *Organometallic Chemistry*, Vol. 41; 2017; pp 48-92.

(10) Ponec, R.; Lendvay, G.; Chaves, J. Structure and bonding in binuclear metal carbonyls from the analysis of domain averaged Fermi holes. I. $Fe_2(CO)_9$ and $Co_2(CO)_8$. *J. Comput. Chem.* **2008**, *29* (9), 1387-1398. DOI: https://doi.org/10.1002/jcc.20894.

(11) Reinhold, J.; Kluge, O.; Mealli, C. Integration of Electron Density and Molecular Orbital Techniques to Reveal Questionable Bonds: The Test Case of the Direct Fe−Fe Bond in $Fe_2(CO)_9$. *Inorg. Chem.* **2007**, *46* (17), 7142-7147. DOI: 10.1021/ic700390v.

(12) Reinhold, J.; Barthel, A.; Mealli, C. Effects of the bridging ligands on the molecular and electronic structure of $Fe_2(CO)_9$ derivatives. *Coord. Chem. Rev.* **2003**, *238-239*, 333-346. DOI: https://doi.org/10.1016/S0010-8545(02)00282-5.

(13) Hunstock, E.; Mealli, C.; Calhorda, M. J.; Reinhold, J. Molecular Structures of $M_2(CO)_9$ and $M_3(CO)_{12}$ (M = Fe, Ru, Os): New Theoretical Insights. *Inorg. Chem.* **1999**, *38* (22), 5053-5060. DOI: 10.1021/ic9905289.

(14) Reinhold, J.; Hunstock, E.; Mealli, C. Is there a direct Fe-Fe bond in $Fe_2(CO)_9$? *New J. Chem.* **1994**, *18* (4), 465-471.

(15) Rosa, A.; Baerends, E. Metal-Metal Bonding in $Fe_2(CO)_9$ and the Double Bonds $Fe(CO)_4$ $=Fe_2(CO)_8$ and (μ-CO)$=Fe_2(CO)_8$ in $Fe_3(CO)_{12}$ and $Fe_2(CO)_9$. Similarities and Differences in the Organic/Inorganic Isolobal Analogues X = Y (X, Y are CH_2, $Fe(CO)_4$, $Fe_2(CO)_8$, C_2H_4, CO). *New J. Chem.* **1991**, *15* (10-11), 815-829.

(16) Mealli, C.; Proserpio, D. M. A new insight from qualitative MO theory into the problem of the Fe · Fe bond in $Fe_2(CO)_9$. *J. Organomet. Chem.* **1990**, *386* (2), 203-208. DOI: https://doi.org/10.1016/0022-328X(90)85245-T.

(17) Bauschlicher, C. W. On the bonding in $Fe_2(CO)_9$. *J. Chem. Phys.* **1986**, *84* (2), 872-875. DOI: 10.1063/1.450532.

(18) Freund, H.-J.; Hohlneicher, G. Calculation of transition metal compounds using an extension of the CNDO formalism. *Theoret. Chim. Acta* **1979**, *51* (2), 145-162. DOI: 10.1007/BF00554098.
(19) Freund, H.-J.; Dick, B.; Hohlneicher, G. Calculation of transition metal compounds using an extension of the CNDO-formalism. *Theoret. Chim. Acta* **1980**, *57* (3), 181-207. DOI: 10.1007/BF00554101.
(20) Summerville, R. H.; Hoffmann, R. M_2L_9 complexes. *J. Am. Chem. Soc.* **1979**, *101* (14), 3821-3831. DOI: https://doi.org/10.1021/ja00508a019.
(21) Whitmire, K. H.; Guzman-Jimenez, I. Y.; Saillard, J.-Y.; Kahlal, S. Synthesis, characterization, structural and theoretical analysis of a series of electron deficient, monomeric thallium iron carbonylate isostructural and isolobal to diiron nonacarbonyl. *J. Organomet. Chem.* **2000**, *614-615*, 243-254. DOI: https://doi.org/10.1016/S0022-328X(00)00629-X.
(22) Green, J. C.; Green, M. L. H.; Parkin, G. The occurrence and representation of three-centre two-electron bonds in covalent inorganic compounds. *Chem. Commun.* **2012**, *48* (94), 11481-11503, 10.1039/C2CC35304K. DOI: 10.1039/C2CC35304K.
(23) Speyer, E.; Wolf, H. Über die Bildungsweise von Eisen-nonacarbonyl aus Eisen-pentacarbonyl. *Ber. Deut. Chem. Ges.* **1927**, *60* (6), 1424-1425. DOI: https://doi.org/10.1002/cber.19270600626.
(24) Cotton, F. A.; Troup, J. M. Accurate determination of a classic structure in the metal carbonyl field: nonacarbonyldi-iron. *J. Chem. Soc. Dalton Trans.* **1974**, (8), 800-802, 10.1039/DT9740000800. DOI: 10.1039/DT9740000800.
(25) Schmitt, M.; Mayländer, M.; Goost, J.; Richert, S.; Krossing, I. Chasing the Mond Cation: Synthesis and Characterization of the Homoleptic Nickel Tetracarbonyl Cation and its Tricarbonyl-Nitrosyl Analogue. *Angew. Chem. Int. Ed.* **2021**, *60* (27), 14800-14805. DOI: https://doi.org/10.1002/anie.202102216.
(26) Morton, J. R.; Preston, K. F. EPR spectra and structures of three binuclear nickel carbonyls trapped in a krypton matrix: $Ni_2(CO)_8^+$, $Ni_2(CO)_7^-$, and $Ni_2(CO)_6^+$. *Inorg. Chem.* **1985**, *24* (21), 3317-3319. DOI: 10.1021/ic00215a003.
(27) Cui, J.; Wang, G.; Zhou, X.; Chi, C.; Hua Li, Z.; Liu, Z.; Zhou, M. Infrared photodissociation spectra of mass selected homoleptic nickel carbonyl cluster cations in the gas phase. *Phys. Chem. Chem. Phys.* **2013**, *15* (25), 10224-10232, 10.1039/C3CP44588G. DOI: 10.1039/C3CP44588G.
(28) Liu, Z.; Bai, Y.; Li, Y.; He, J.; Lin, Q.; Zhang, F.; Wu, H.-S.; Jia, J. Triply Carbonyl-Bridged $Ni_2(CO)_5$ Featuring Triple Three-Center Two-Electron Ni—C–Ni Bonds Instead of Ni≡Ni Triple Bond. *Inorg. Chem.* **2020**, *59* (20), 15365-15374. DOI: 10.1021/acs.inorgchem.0c02334.
(29) Hornung, J.; Muhr, M.; Gemel, C.; Fischer, R. A. All-zinc coordinated nickel-complexes as molecular mimics for NiZn catalyst surfaces, a density functional theory study. *Dalton Trans.* **2019**, *48* (31), 11743-11748, 10.1039/C9DT02005E. DOI: 10.1039/C9DT02005E.
(30) Grunze, M.; Golze, M.; Hirschwald, W.; Freund, H. J.; Pulm, H.; Seip, U.; Tsai, M. C.; Ertl, G.; Küppers, J. π-Bonded N_2 on Fe(111): The Precursor for Dissociation. *Phys. Rev. Lett.* **1984**, *53* (8), 850-853. DOI: 10.1103/PhysRevLett.53.850.
(31) Cotton, F. A.; Curtis, N. F.; Harris, C. B.; Johnson, B. F. G.; Lippard, S. J.; Mague, J. T.; Robinson, W. R.; Wood, J. S. Mononuclear and Polynuclear Chemistry of Rhenium (III): Its Pronounced Homophilicity. *Science* **1964**, *145* (3638), 1305-1307. DOI: doi:10.1126/science.145.3638.1305.
(32) Lawton, D.; Mason, R. The Molecular Structure of Molybdenum(II) Acetate. *J. Am. Chem. Soc.* **1965**, *87* (4), 921-922. DOI: 10.1021/ja01082a046.

(33) Cotton, F. A. Centenary Lecture. Quadruple bonds and other multiple metal to metal bonds. *Chem. Soc. Rev.* **1975**, *4* (1), 27-53, 10.1039/CS9750400027. DOI: 10.1039/CS9750400027.
(34) Cotton, F. A.; Murillo, C. A.; Walton, R. A. *Multiple Bonds between Metal Atoms*; Springer New York, NY, 2005.
(35) Nguyen, T.; Sutton, A. D.; Brynda, M.; Fettinger, J. C.; Long, G. J.; Power, P. P. Synthesis of a Stable Compound with Fivefold Bonding Between Two Chromium(I) Centers. *Science* **2005**, *310* (5749), 844-847. DOI: 10.1126/science.1116789.
(36) Tsai, Y.-C.; Chen, H.-Z.; Chang, C.-C.; Yu, J.-S. K.; Lee, G.-H.; Wang, Y.; Kuo, T.-S. Journey from Mo−Mo Quadruple Bonds to Quintuple Bonds. *J. Am. Chem. Soc.* **2009**, *131* (35), 12534-12535. DOI: 10.1021/ja905035f.
(37) Liu, S.-C.; Ke, W.-L.; Yu, J.-S. K.; Kuo, T.-S.; Tsai, Y.-C. An Electron-Rich Molybdenum–Molybdenum Quintuple Bond Spanned by One Lithium Atom. *Angew. Chem. Int. Ed.* **2012**, *51* (26), 6394-6397. DOI: https://doi.org/10.1002/anie.201200122.
(38) Carrasco, M.; Curado, N.; Maya, C.; Peloso, R.; Rodríguez, A.; Ruiz, E.; Alvarez, S.; Carmona, E. Interconversion of Quadruply and Quintuply Bonded Molybdenum Complexes by Reductive Elimination and Oxidative Addition of Dihydrogen. *Angew. Chem. Int. Ed.* **2013**, *52* (11), 3227-3231. DOI: https://doi.org/10.1002/anie.201209064.
(39) Frenking, G. Building a Quintuple Bond. *Science* **2005**, *310* (5749), 796-797. DOI: 10.1126/science.1120281 (acccessed 2022/11/22).
(40) Muhr, M.; Bühler, R.; Liang, H.; Gilch, J.; Jandl, C.; Kahlal, S.; Saillard, J.-Y.; Gemel, C.; Fischer, R. A. C−H and Si−H Activation Reactions at Ru/Ga Complexes: A Combined Experimental and Theoretical Case Study on the Ru−Ga Bond. *Chem. Eur. J.* **2022**, *28* (54), e202200887. DOI: https://doi.org/10.1002/chem.202200887.
(41) Schütz, M.; Gemel, C.; Muhr, M.; Jandl, C.; Kahlal, S.; Saillard, J.-Y.; Fischer, R. A. Exploring Cu/Al cluster growth and reactivity: from embryonic building blocks to intermetalloid, open-shell superatoms. *Chem. Sci.* **2021**, *12* (19), 6588-6599, 10.1039/D1SC00268F. DOI: 10.1039/D1SC00268F.
(42) Schütz, M.; Gemel, C.; Klein, W.; Fischer, R. A.; Fässler, T. F. Intermetallic phases meet intermetalloid clusters. *Chem. Soc. Rev.* **2021**, *50* (15), 8496-8510, 10.1039/D1CS00286D. DOI: 10.1039/D1CS00286D.
(43) Mayer, K.; Weßing, J.; Fässler, T. F.; Fischer, R. A. Intermetalloid Clusters: Molecules and Solids in a Dialogue. *Angew. Chem. Int. Ed.* **2018**, *57* (44), 14372-14393. DOI: doi:10.1002/anie.201805897.
(44) Steinke, T.; Gemel, C.; Winter, M.; Fischer, R. A. The Clusters $[M_a(ECp^*)_b]$ (M=Pd, Pt; E=Al, Ga, In): Structures, Fluxionality, and Ligand Exchange Reactions. *Chem. Eur. J.* **2005**, *11* (5), 1636-1646. DOI: 10.1002/chem.200400959.
(45) Heiß, P.; Hornung, J.; Gemel, C.; Fischer, R. A. A combinatorial coordination-modulated approach to all-hydrocarbon-ligated intermetallic clusters. *Chem. Commun.* **2022**, *58* (27), 4332-4335, 10.1039/D2CC00396A. DOI: 10.1039/D2CC00396A.
(46) Gonzalez-Gallardo, S.; Bollermann, T.; Fischer, R. A.; Murugavel, R. Cyclopentadiene based low-valent group 13 metal compounds: ligands in coordination chemistry and link between metal rich molecules and intermetallic materials. *Chem. Rev.* **2012**, *112* (6), 3136-3170. DOI: 10.1021/cr2001146.
(47) Steinke, T.; Gemel, C.; Cokoja, M.; Winter, M.; Fischer, R. A. AlCp* as a directing ligand: C--H and Si--H bond activation at the reactive intermediate $[Ni(AlCp^*)_3]$. *Angew. Chem. Int. Ed.* **2004**, *43* (17), 2299-2302. DOI: 10.1002/anie.200353114.
(48) Weßing, J.; Ganesamoorthy, C.; Kahlal, S.; Marchal, R.; Gemel, C.; Cador, O.; Da Silva, A. C. H.; Da Silva, J. L. F.; Saillard, J.-Y.; Fischer, R. A. The Mackay-Type Cluster

[$Cu_{43}Al_{12}$](Cp*)$_{12}$: Open-Shell 67-Electron Superatom with Emerging Metal-Like Electronic Structure. *Angew. Chem. Int. Ed.* **2018**, *57* (44), 14630-14634. DOI: 10.1002/anie.201806039.
(49) Hoffmann, R. Building Bridges Between Inorganic and Organic Chemistry (Nobel Lecture). *Angew. Chem. Int. Ed.* **1982**, *21* (10), 711-724. DOI: https://doi.org/10.1002/anie.198207113.
(50) Elian, M.; Chen, M. M. L.; Mingos, D. M. P.; Hoffmann, R. Comparative bonding study of conical fragments. *Inorg. Chem.* **1976**, *15* (5), 1148-1155. DOI: 10.1021/ic50159a034.
(51) Hornung, J.; Weßing, J.; Jerabek, P.; Gemel, C.; Pöthig, A.; Frenking, G.; Fischer, R. A. Suppressed Phosphine Dissociation by Polarization Effects on the Donor–Acceptor Bonds in [$Ni(PEt_3)_{4-n}(ECp^*)_n$] (E = Al, Ga). *Inorg. Chem.* **2018**, *57* (20), 12657-12664. DOI: 10.1021/acs.inorgchem.8b01817.
(52) Fischer, R. A.; Weiß, J. Coordination Chemistry of Aluminum, Gallium, and Indiumat Transition Metals. *Angew. Chem. Int. Ed.* **1999**, *38*, 2830-2850.
(53) Uhl, W.; Benter, M.; Melle, S.; Saak, W.; Frenking, G.; Uddin, J. Synthesis and Structure of [$Ni\{Ga{-}C(SiMe_3)_3\}_4$] and Quantum-Chemical Verification of Strong π Back-Bonding in the Model Compounds [$Ni(EMe)_4$] (E = B, Al, Ga, In, Tl). *Organometallics* **1999**, *18* (19), 3778-3780. DOI: 10.1021/om990417h.
(54) Uddin, J.; Boehme, C.; Frenking, G. Nature of the Chemical Bond between a Transition Metal and a Group-13 Element: Structure and Bonding of Transition Metal Complexes with Terminal Group-13 Diyl Ligands ER (E = B to Tl; R = Cp, $N(SiH_3)_2$, Ph, Me). *Organometallics* **2000**, *19* (4), 571-582. DOI: 10.1021/om990936k.
(55) Uddin, J.; Frenking, G. Energy Analysis of Metal-Ligand Bonding in Transition Metal. *J. Am. Chem. Soc.* **2001**, *123*, 1683-1693.
(56) Weiß, D.; Winter, M.; Fischer, R. A.; Yu, C.; Wichmann, K.; Frenking, G. [$Pt_2(GaCp^*)_2(\mu_2\text{-}GaCp^*)_3$]: structure and bonding situation of the first homoleptic platinum complex with terminal and bridging Cp*Ga ligands. *Chem. Commun.* **2000**, (24), 2495-2496, 10.1039/B008133G. DOI: 10.1039/B008133G.
(57) Muhr, M.; Hornung, J.; Weßing, J.; Jandl, C.; Gemel, C.; Fischer, R. A. Formation of a Propeller-Shaped Ni_4Ga_3 Cluster Supported by Transmetalation of Cp* from Ga to Ni. *Inorg. Chem.* **2020**, *59* (7), 5086-5092. DOI: 10.1021/acs.inorgchem.0c00344.
(58) Molon, M.; Gemel, C.; Fischer, R. A. Organogallium- and organozinc-rich palladium and platinum clusters. *Dalton Trans.* **2014**, *43* (8), 3114-3120. DOI: 10.1039/c3dt53003e.
(59) Molon, M.; Bollermann, T.; Gemel, C.; Schaumann, J.; Fischer, R. A. Mixed phosphine and group-13 metal ligator complexes [$(PR_3)_aM(ECp^*)_b$] (M = Mo, Ni; E = Ga, Al; R = C_6H_5, cyclo-C_6H_{11}, CH_3). *Dalton Trans.* **2011**, *40* (40), 10769-10774, 10.1039/C1DT10583C. DOI: 10.1039/C1DT10583C.
(60) Buchin, B.; Steinke, T.; Gemel, C.; Cadenbach, T.; Fischer, R. A. Synthesis and Characterization of the Novel AlI Compound Al(C_5Me_4Ph): Comparison of the Coordination Chemistry of Al(C_5Me_5) and Al(C_5Me_4Ph) at d^{10} Metal Centers). *Z. anorg. allg. Chemie* **2005**, *631* (13- 14), 2756-2762. DOI: doi:10.1002/zaac.200500129.
(61) Cordero, B.; Gómez, V.; Platero-Prats, A. E.; Revés, M.; Echeverría, J.; Cremades, E.; Barragán, F.; Alvarez, S. Covalent radii revisited. *Dalton Trans.* **2008**, (21), 2832-2838, 10.1039/B801115J. DOI: 10.1039/B801115J.
(62) Antsiburov, I.; Schütz, M.; Bühler, R.; Muhr, M.; Stephan, J.; Gemel, C.; Klein, W.; Kahlal, S.; Saillard, J.-Y.; Fischer, R. A. All-Hydrocarbon Ligated Superatomic Gold/Aluminium Clusters. *Submitted* **2023**.
(63) Albright, T. A.; Burdett, J. K.; Whangbo, M.-H. *Orbital Interactions in Chemistry*; Wiley, 2013.

(64) Grimme, S.; Ehrlich, S.; Goerigk, L. Effect of the damping function in dispersion corrected density functional theory. *J. Comput. Chem.* **2011**, *32* (7), 1456-1465. DOI: doi:10.1002/jcc.21759.
(65) Grimme, S. Semiempirical GGA-type density functional constructed with a long-range dispersion correction. *J. Comput. Chem.* **2006**, *27* (15), 1787-1799. DOI: https://doi.org/10.1002/jcc.20495.
(66) Mingos, D. M. P.; Wales, D. J. *Introduction to Cluster Chemistry*; Prentice Hall, 1990.
(67) von Hänisch, C. K. F.; Üffing, C.; Junker, M. A.; Ecker, A.; Kneisel, B. O.; Schnöckel, H. [$As_2(AlCp^*)_3$]—A Compound with a Polyhedral As_2Al_3 Framework. *Angew. Chem. Int. Ed. Engl.* **1996**, *35* (23-24), 2875-2877. DOI: https://doi.org/10.1002/anie.199628751.
(68) Ganesamoorthy, C.; Krüger, J.; Glöckler, E.; Helling, C.; John, L.; Frank, W.; Wölper, C.; Schulz, S. Comprehensive Study on Reactions of Group 13 Diyls with Tetraorganodipentelanes. *Inorg. Chem.* **2018**, *57* (15), 9495-9503. DOI: 10.1021/acs.inorgchem.8b01489.
(69) Dabringhaus, P.; Zedlitz, S.; Giarrana, L.; Scheschkewitz, D.; Krossing, I. Low-Valent M_xAl_3 Cluster Salts with Tetrahedral $[SiAl_3]^+$ and Trigonal-Bipyramidal $[M_2Al_3]^{2+}$ Cores (M=Si/Ge). *Angew. Chem. Int. Ed.* **2023**, *62* (8), e202215170. DOI: https://doi.org/10.1002/anie.202215170.